

A 2.75 D FINITE ELEMENT MODEL OF 3 D FRACTURE NETWORK SYSTEMS

Sylvia Moenickes^{1,2}, Takeo Taniguchi³, René Kaiser¹, Werner Zielke¹

¹*Institute for Fluid Mechanics, ISEB, Universität Hannover, Hannover, Germany.*

²*moenickes@hydromech.uni-hannover.de*

³*Faculty of Environmental Science and Technology, Okayama University, Okayama, Japan*

ABSTRACT

The simulation of fluid flow and heat transport in fracture network systems requires new grid generation techniques. A fractured subsurface domain may be regarded as a convex 3 d domain split up into convex subdomains. When it comes to hexahedrally meshing it there is still no method which provides overall simplicity, uniqueness, and robustness, and furthermore good mesh quality near those fracture planes as they govern the phenomena. For these cases we propose 2.75 d meshes. The basic idea is that the regions with steady state conditions need not be considered and, consequently they need not be meshed at all. Those regions are located far from the fractures. Accordingly, the 2.75 d mesh is a skeleton of 3 d elements covering the fracture planes in the domain. These can thus be analytically computed as layered hexahedral elements. Pre-requisites are a topological analysis of the domain and expertise in fluid dynamics in order to properly decide about the space to be omitted.

Keywords: mesh generation, hexahedral mesh, composed domain, fracture network

1. INTRODUCTION

This grid generation method has been developed to meet the needs arising in fluid flow simulations of fracture network systems. The case to be treated is the geothermal research site Soultz-sous-forêts in France (see figure 1 and (1)). At a depth of 3500 m hot dry granite rock at 165 °C was found. This domain of about 5 km³ consists of seven main fractures in a porous matrix. Geological analysis showed that these fractures can be regarded as planes which are not only highly intersecting but also often at extremely small angles (see figure 2). Both an injection well and an extraction well were drilled in order to provide heated water. Back at the surface, the water temperature of about 140 °C is used to generate more than 10 MWe. For optimisation of energy production it is necessary to fully understand the flow regime. This is attained by FEM - simulations of the fluid flow, of a tracer and heat transport for which different models have been developed: a) discrete modeling, b) continuum or multicontinuum approach or c) hybrid models, see (2) and

(3) for details. Discrete as well as hybrid models require as input data the geometry of the considered domain and its fractures. For discrete models two different approaches have been pursued: In the first approach the fractures and matrix are represented as finite elements of the same dimension (equidimensional modelling), in the second one the dimension of the fractures' finite elements is reduced by one omitting the direction vertical to the fracture plane. This procedure has the advantage of keeping the unknown thickness of the fracture as a parameter and thus reduces the discretization scale needed for stability and correctness of the simulations. A pre-requisite for these simulations in fracture network systems is the hexahedral FEM - grid whose generation will be discussed subsequently.

2. OUTLINE

Generally and abstractly spoken, meshing this domain means meshing a convex 3 d domain which is split up

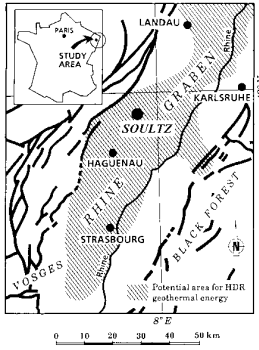


Figure 1: The research side Soutz-sous-forêts

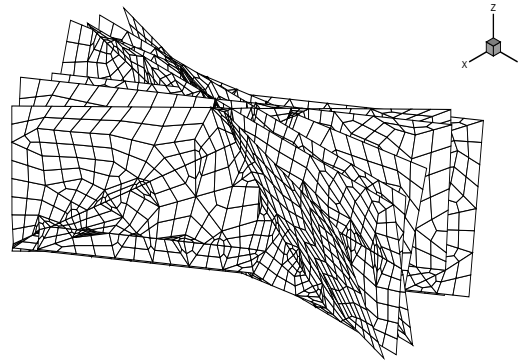


Figure 2: A model of the fracture network

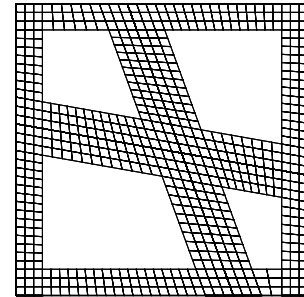
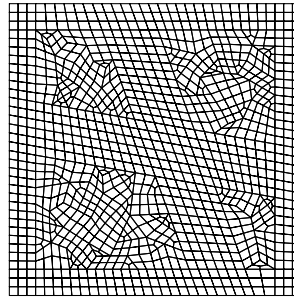
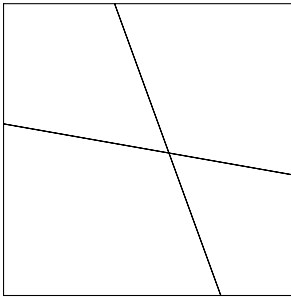


Figure 3: Outline of the method's idea

into convex subdomains by idealized planes. Whereas a focus on the given case illuminates the concrete, special features needed: The experience in fluid simulation for fracture network systems shows that the fluid flow through the fractures themselves is dominant while that through the adjacent rock matrix may be neglected. For tracer or heat flow the processes in the fractures are still prevailing, being influenced by the rock matrix in their close vicinity only. Steady state conditions are found in the rock matrix more distant to the fractures. As a result of this a high finite element mesh quality is desired especially near the fractures. In other words: far from the fractures an excellent mesh quality of even a mesh is not necessarily needed. Omitting the inside of all subdomains reduces the mesh to a skeleton of hexahedra covering the fracture planes. This offers a possibility for simplifying and accelerating the simulation. The amount of mesh that may be omitted solely depends on the physical properties of the rock matrix and the fluid: the transmissibility, the heat conductivity, and therefore the porosity.

The focus on the given case raises one last question: how can the numerical stability be increased for those finite elements of the rock matrix containing consti-

tutionally small angles? Those fractures that intersect under an exceedingly small angle produce an extended zone of intermediate porosity. This porosity is attributed to all of the elements close to the intersection line. In doing so, on the one hand, a more realistic physical model is obtained, and on the other hand the numerical stability of these less well shaped elements is improved. Besides these two features simplicity, uniqueness, and robustness are required.

A closer look at the available hexahedral meshing methods shows: the advancing front method and its family for 3d hexahedral meshing do not provide uniqueness and suffer from a lack of closure procedures. Blocking methods are not recommended due to the manual effort needed. Finally, tetrahedral meshing followed by hexahedration (see (4)) cannot improve the mesh quality generated by the triangulation, but fulfills the other requirements stated above. Thus it can be taken as the starting point for the development of the new mesh generator.

In order to ensure numerical stability and to generate better numerical results, layers of hexahedra are favorable to tetrahedra based meshing methods. This fact leads to the simple idea of providing layered hexahedral elements covering the fracture prior to meshing

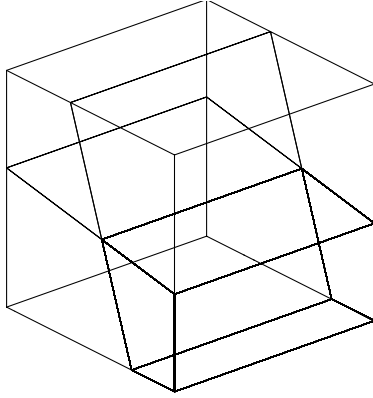


Figure 4: The example: A cube with two fractures

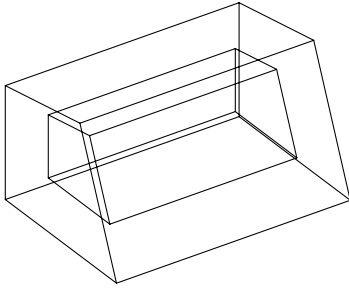


Figure 5: Shrinking of one subdomain

the inside with a set of tetrahedration and hexahedration, see figure 3b for a 2d equivalent. As has been mentioned above, the mesh may be reduced to the skeleton formed by the layered hexahedral elements covering the fractures. This will be referred to as 2.75 d mesh (see figure 3c for a 2d equivalent).

3. TECHNIQUE

The realization of this grid generation idea can be trisected: topological analysis, shrinking, and meshing. In order to illustrate each step a simple 3d cube including two fractures is used, see figure 4.

At first, a topological analysis of the domain is made. For this purpose the fracture planes as well as each of the six planes of the bounding cube are described by a collection of triangles. The whole domain is regarded as a set of subdomains separated by the fractures, as each fracture and each boundary plane is regarded as a set of plane segments separated by the lines of intersection with other planes. For the cube including two fractures the domain is transformed into four subdomains, the two fractures into four fracture plane segments, and the six boundaries into sixteen boundary

plane segments. Finally, the subdomains are described by the sum of the bounding plane segments. Any subdomain of this example is described by six plane segments, a hexahedron, while in general it may be any polyhedron.

In the second step each subdomain is treated separately. For each subdomain all related bounding plane segments are taken and this convex hull 'shrunk' into the subdomain, shown in figure 5. As it is assumed that no more than three planes intersect at one point, the shrunk hull can be derived by calculating the intersection of parallelly shifted planes. Differing from the prevalent shrinking method (using the centre of gravity) this procedure provides a constant distance to the hull planes. This distance should be defined according to the simulation's demands. As a result of the shrinking, the subdomain is divided into two parts. The inside of the shrunk hull will be referred to as 'core' while the remaining space between both hulls will be called the 'skin'. The core has a similar shape as the subdomain. In explicit terms, comparing the analogous boundary plane segments of the original and the shrunk hull, the shrunk polygon segments have the same angles as do those of the original polygon but generally have different lengths.

In the last step, the components of the domain are meshed. These are each subdomain's skin part, its core part and the fracture elements.

In turn each skin can be split into three types of partitions, see figure 6:

1. a parallelepiped, thus a hexahedron, at each vertex where three planes meet, consequently omitting the vertices on the edges or on plane segments
2. a hexahedral prismatoid at each edge that connects two of the vertices described in 1
3. a prismatoid at each plane segment, with a polygonal basis and top and a set of quadrilateral faces at the sides

The shape of the plane segment prismatoid depends on the location and particularly on the angle of the fracture intersections. It is meshed as can be seen from figure 8 and 7 as follows: at first the polygonal boundary of the base plane segment is enriched in nodes and a 2d Delaunay triangulation is applied (see 8 a). This is the starting point for an iterative mesh optimisation: The total length of the sides of each triangle is calculated. If now the greatest length exceeds some given threshold, a node will be inserted dividing the longest edge of the associated triangle and a remeshing takes place. The final iteration (see 8 b) is followed by a quadrangulation using either (5) or (6), see 8c.

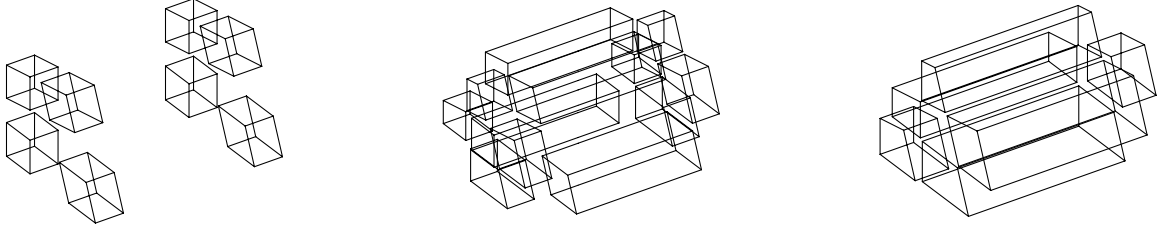


Figure 6: Types of partitions in the skin of each subdomain

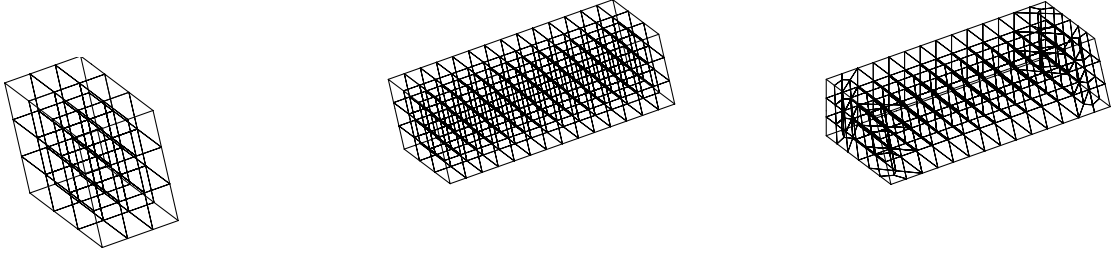


Figure 7: Types of 3d meshing in the skin

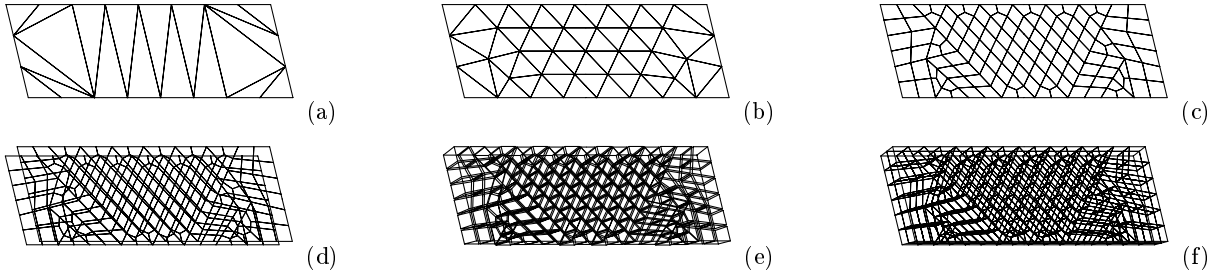


Figure 8: Procedure of plane segment meshing

(5) is a mere subdivision of each triangle into three quadrilaterals, while (6) introduces different geometric coefficients in order to join most of the triangles by pairs and subdivide the remaining triangles into three quadrilaterals and the resulting pairs of triangles into four quadrilaterals. The generated quadrilateral mesh is projected onto the top face of the prismatoid that has been derived by shrinking (see 8d). This is done as follows starting from the fact that the base plane segment and the top plane segment are bound by polygons having the same number of nodes. The nodes that have been inserted into the base plane segment during the iteration described above are mapped topologically. Connecting both meshes yields a hexahedral mesh of the plane segment prismatoid (see 8e). The resulting hexahedra are subdivided vertically to the plane segment according to the desired number of layers of matrix elements on the fractures (see 8f).

The shape of the edge prismatoid mainly depends on

the angle between the two edge originating planes. For consistency reasons, the nodes created on the edge during the meshing of the plane prismatoid are included as points where the prismatoid bar is sliced into smaller hexahedra, see figure 7. These latter ones are again subdivided according to the desired number of layers but this time in two directions parallel to each of the originating planes. Finally, the shape of the vertex prismatoid is completely defined by the angles between the three intersecting planes and is solely treated by three directional subdivision according to the desired number of hexahedra layers, see figure 7.

The last step in the meshing process is the quadrilateration of the fractures themselves as can be seen in figure 9. The above splitting of the skin parts into edge, vertex and plane parts is equivalent to a splitting of the fractures which agrees with both neighboring subdomains for each fracture. Consequently, a 2d version of the skin meshing process takes place: the edges as

well as the vertex parts result in quadrilaterals that are further subdivided into layered FEM quadrilaterals. The remaining polygonal plane is meshed as shown in figures 8a through 8c.

As explained in section 2, one final measure should be taken during the last step in order to enhance the mesh for fracture network flow simulations: The edge prismatoids and the vertex parallelepipeds suffering from a small angle between the intersecting planes are allocated their own material characteristics and thus different from that of the subdomain they belong to. The material properties can be manually adjusted.

The result for the case domain can be seen in figure 10. All of the meshing can be reduced to generating the 2d fracture elements, see (7). This yields a 2.5 d fracture network model that still provides the smoothness of 2d elements at the intersection lines. It is widely applied to fluid flow and mass transport simulations that neglect the influence of the rock matrix. The result of the meshing can as well be extended to a full 3d mesh by including the core parts. In that case, for each subdomain the top faces of all plane prismatoids must be collected in the state of triangular meshes which implies the mapping of the nodes of the base plane segment (8b) onto the top plane segment. This scatter plot can then be meshed using a 3d Delaunay tetrahedration which is followed by the hexahedration, see figure 11 and (8).

4. APPLICATIONS AND CONCLUSIONS

Two applications of the algorithm explained will be illustrated. The first is the Sauty case study, see (9). It is a simple single-fracture domain whose geometry can be seen in figure 12. The hatched planes represent the inlet and outlet. The Sauty case has often been used to analyse fluid, tracer and heat flow. The second application considers the Soultz case explained in detail above.

4.1 Sauty-Cube

As one can see from figure 13, the algorithm may be applied to this single-fracture domain as well. The user simply has to make sure that those parts of the space dominated by the processes to be simulated are filled with finite elements. This can be done by extending the amount of shrinking but is restricted to the size of the smallest plane segment.

4.2 Soultz-sous-forêts

The grid generated for the Soultz case can be seen in figures 14 and 15. The first one displays the 2.75 d model. In contrast to this, the second one shows the

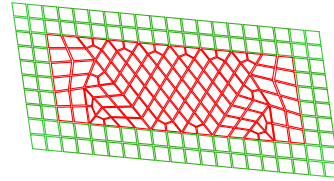


Figure 9: 2 d meshing of an example fracture

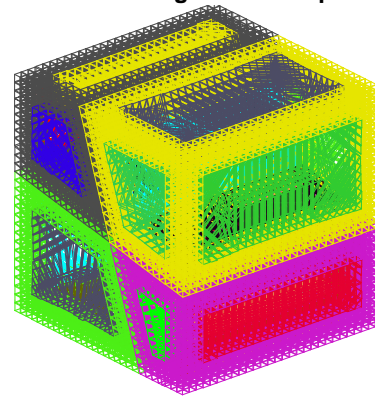


Figure 10: Full 2.75 d meshing of the example cube

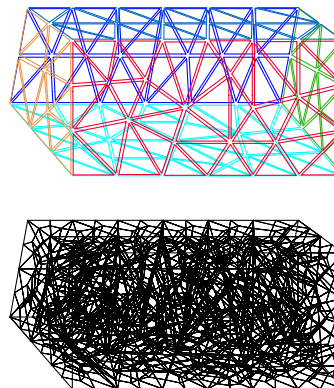


Figure 11: Hexahedration of a core of the example cube

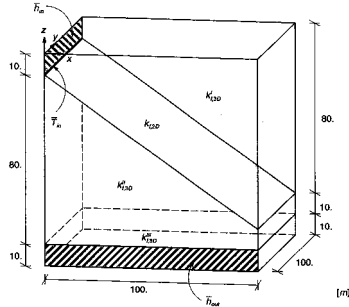


Figure 12: The geometry of the Sauty example

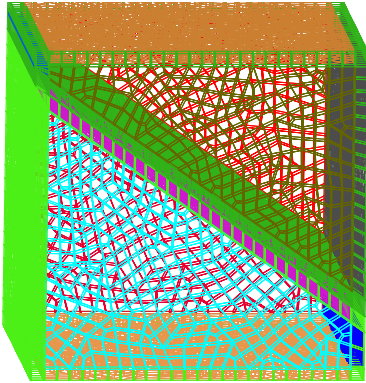


Figure 13: 2.75d meshing of the Sauty example

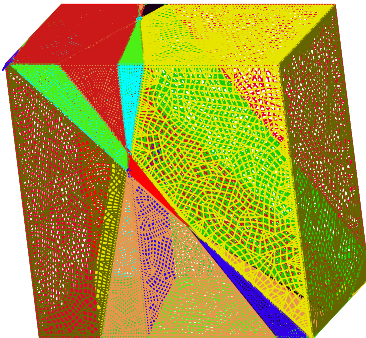


Figure 14: 2.75d meshing of the Sultz case

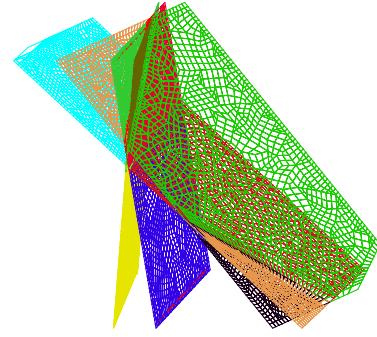


Figure 15: 2.5d meshing of the Sultz case

2.5 d model. That means that the model is reduced to 2d finite elements describing the fracture planes.

4.3 Conclusions

Generally, it is possible to replace a full 3d model of a fractured domain by a 2.75d model. This offers an opportunity to simplify the model while performing accelerated simulations.

The only pre-requisite is the assumption of a steady state condition of the processes considered in those areas of the domain that are not included in the mesh. Consequently, expertise in adapting the thickness of the FEM grid layer around the fractures is needed. This thickness is limited by the smallest plane segment.

Future work will concentrate on improving the mesh. This includes a refinement of the algorithm to allow non-penetrating fractures for far-field simulations and the additional inclusion of non-planar objects such as wells.

5. ACKNOWLEDGEMENTS

This work was conducted at the Universität Hannover and the Okayama University. It was supported by the 'DFG' and by the 'DAAD Doktorandenstipendium im Rahmen des gemeinsamen Hochschulsonderprogramms III von Bund und Ländern'. The authors wish to thank Mr. O. Kolditz and Mr. Th. Rother for their support.

References

- [1] Baria R., Baumgaertner J., Gerard A., Jung R., Garnish J. "European HDR research programme at Soultz-sous-Forêts (France) 1987-1996." *Geothermics*, vol. 28, no. 3, 1999

- [2] 3. Workshop Kluft-Aquifere - Gekoppelte Prozesse in Geosystemen, 2000
- [3] Kolditz O. *Strömung, Stoff- und Wärmetransport im Kluftgestein*. Borntraeger, Stuttgart, 1997
- [4] Taniguchi T., Tomoaki G., Kasper H., Zielke W. "Automatic Grid Adaptation for Subsurface Fluid Flow Problems Application fo Fractured-Porous Reservoirs." *Proceedings XII. International Conference on Computational Methods in Water Resources*. Crete, Greece, 1998
- [5] Everett H., Lenhart W., Overmars M., Shermer T., Urrutia J. "Strictly convex quadrilateralizations of polygons." *Proceedings of the 4th Canadian Conference on Computational Geometry*, pp. 77-83. 1992
- [6] Lo S.H. "Generating quadrilateral elements on plane and over curved surfaces." *Computers and Structures*, vol. 31, no. 3, 421-426, 1989
- [7] Rother T., Kolditz O., Taniguchi T. "Grid Generation of Fractured-Porous Aquifers." *Proceedings 7th International Conference on Numerical Grid Generation in Computational Field Simulations*. Whistler, Canada, 2000
- [8] Taniguchi T. *Automatic Mesh generation for FEM - Use of Delaunay Triangulation*. Morikita Publishing, 1991. In Japanese
- [9] Barlag C. *Adaptive Methoden zur Modellierung von Stofftransport im Kluftgestein*. Ph.D. thesis, Universität Hannover, 1997. ISSN 0177 - 9028